MDPI

Article

Risk Assessment for Critical Flood Height of Pedestrian Escape in Subway Station

Yi Tang [1], Tianzhong Zhou [2], Youxin Zhong [2], Shengbin Hu [2], Jing Lin [2], Zhiyu Lin [1], Hongwei Liu [1], Baohua Liu [1], Yanlin Zhao [3], Yixian Wang [4] and Hang Lin [1,*]

1   School of Resources and Safety Engineering, Central South University, Changsha 410083, China
2   Nanning Rail Transit Co., Ltd., Nanning 530028, China
3   School of Energy and Safety Engineering, Hunan University of Science and Technology, Xiangtan 411201, China
4   School of Civil Engineering, Hefei University of Technology, Hefei 230009, China
*   Correspondence: hanglin@csu.edu.cn

Abstract: The escape of pedestrians in the subway station is hampered by floods created by heavy rain. In order to explore the critical flood level in a subway station so that pedestrians can escape safely, the case study of the Mingxiu Road subway station in Nanning, China, was conducted using numerical simulation techniques. In total, 30 groups of sample pedestrians with different walking speeds and numbers were randomly generated by the Monte Carlo method, and 3D simulation software was used for escape simulation. The simulated escape data were put into the SVM model, and the maximum pedestrian capacity and minimum speed of pedestrians were solved successfully with different conditions of the Mingxiu Road subway station. Then, a 1:1 contour model of the pedestrian was constructed to simulate the flood resistance of the pedestrian escaping at the minimum speed. The flood resistance and the friction force between the pedestrian and the ground were compared to calculate the critical escape flood level height, and the critical escape flood level height of an adult, child, and elder was 87.4 cm, 75.5 cm, and 83.0 cm, respectively.

Keywords: Monte Carlo method; 3D simulation; maximum pedestrian capacity; minimum speed of safe escape; critical escape flood level height

1. Introduction

In recent years, the rapid development of social economy and production technology has led to the rapid expansion of the urban construction scale [1–3], and the surface of the city is not sufficient for all kinds of infrastructure to be built [4–6]. Therefore, the development of underground space is an excellent direction for the sustainable development of the city. However, compared to the spacious surface, the underground space is a very closed place [7–9], with only a few auxiliary facilities (air shafts) and individual pedestrian entrances and exits, which are used by pedestrians connecting the underground space and the surface. In this case, once a disaster occurs, the space and time for pedestrians to escape will be very limited [10–12]. Compared with the surface, the characteristics of the underground space have three points [13,14]: (1) The underground space is very closed. It is only connected to the outside through a small number of water outlets, and drainage can only be carried out mechanically. (2) The interior structure of the underground space is complex, and the various buildings inside occupy a large area. (3) It is difficult to evacuate pedestrians safely [15]. Due to the complex internal structure of the underground space and the low terrain, the flood flow into the subway station cannot be eliminated in time [16–18], which poses a great threat to pedestrian safety [19,20]. In addition, compared with the movement on the surface, escaping from the underground space to the surface requires overcoming gravity to work, which costs more physical energy, and it is more difficult for pedestrians to evacuate safely [21].

Since the development of urban underground space, many accidents have occurred [22–24]. In January 2006, an underground garage in Brazil was flooded with a maximum flood depth of 2.2 m, killing six pedestrians [25]. Due to the closed structure of the underground space, pedestrians need to spend more time escaping when safety accidents such as floods occur in subway stations. Many scholars have carried out relevant studies on subway pedestrian evacuation. Yukawa et al. [26] proposed a method to evaluate evacuation plans for large urban floods based on equilibrium analysis. Zheng et al. [25] studied the dynamic evacuation of subway pedestrians with flood based on an improved floor-field model. Uno et al. [27] proposed a disaster evacuation simulation system based on a multi-agent model and applied the system to evacuation analysis of urban flood disasters. Simonovic et al. [28] constructed a computer simulation model based on system dynamics to identify human behavior in floods.

The above research, based on the methods of macroscopic simulation, dynamics, and evacuation model, has many valuable suggestions and experiences for pedestrian escape in subway stations with flood attacks. However, it must be noted that the rising flood in the subway station will cause great psychological pressure on the pedestrian, thus triggering a series of stampedes. In addition, the buoyancy and resistance generated by the flood will seriously hinder the normal escape of the pedestrian. When the flood height exceeds a critical level, the pedestrian will not be able to escape safely. Therefore, if the critical escape flood height of the pedestrian can be calculated, the pressure of evacuation will be relieved.

This paper proposed a method to calculate the critical flood height for the evacuation of pedestrians in subway stations. This method can calculate the maximum capacity and minimum escape speed of pedestrians in subway stations with different conditions and the critical flood height for pedestrians to achieve a safe escape. It is of practical significance.

2. Model and Method

2.1. Model of Subway Station

We used the Nanning Mingxiu Road Subway Station as an engineering model (Figures 1–7). Mingxiu Road station is a transfer station located in the bustling area of Nanning city. It consists of a surface plaza, 3 underground floors, and 12 exits leading to the city streets, forming a huge underground transportation system. The first basement floor is the one with the largest scale and the most commercial shops, named the property floor, and the second basement floor is the station hall floor, which is used for transfer and crowds entering the station. The third underground layer is the platform layer, which is used by pedestrians waiting for the arrival of the subway and entering the subway [29]. In addition, to ensure that the model can succinctly and intuitively reflect the pedestrian evacuation situation succinctly and intuitively, some contents need to be simplified. First of all, the components such as walls and columns that will hinder the observation of the evacuation process need to be simplified, they will be regarded as two-dimensional obstacles, and the height attribute will be removed. The elevator was deemed unusable. In addition, only public areas accessible to pedestrians are considered, and various facilities such as cable rooms and power distribution rooms in subway stations are not considered. The final model planes of each layer are shown in Figures 1–6. According to relevant regulations, the design of the station should ensure that the evacuation from the farthest location on the platform to a safe location can be completed in 6 min or less. Therefore, assuming that the pedestrian response time is 30 s, all pedestrians should be evacuated to the surface safety within $360 - 30 = 330$ (s) [30].
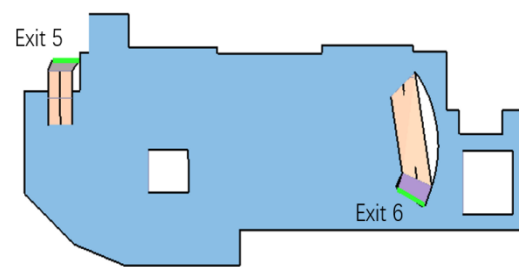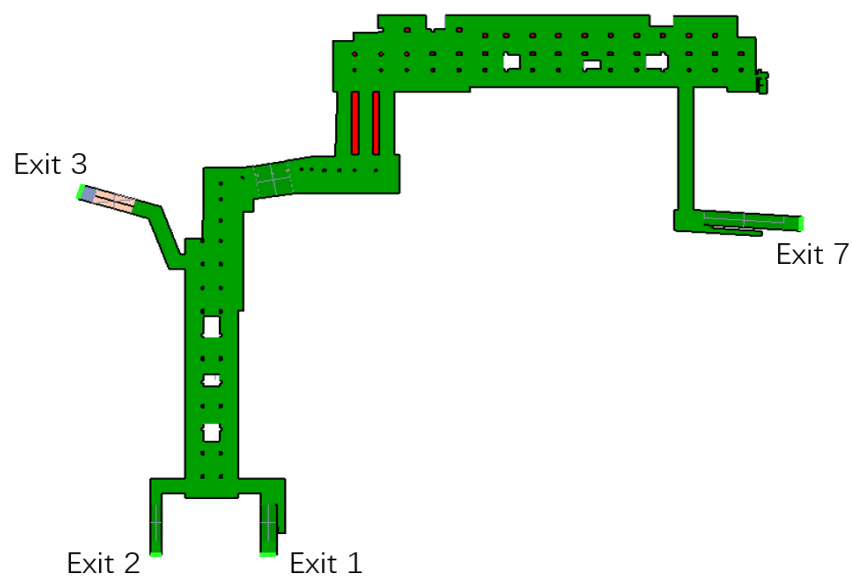
Figure 1. Surface model of the sunken square.
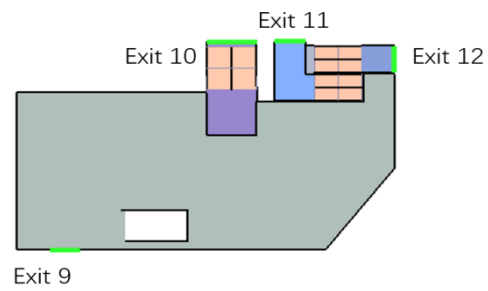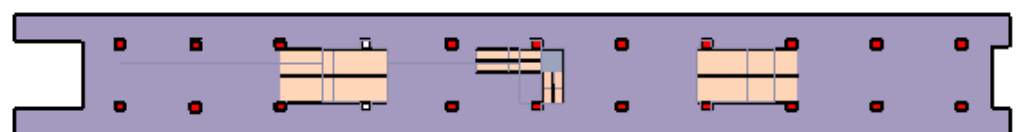

Figure 2. Surface model and export instructions.
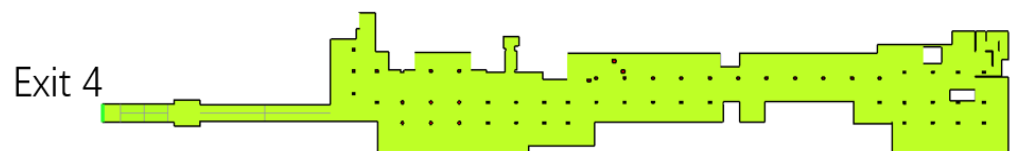
Figure 3. Property layer model diagram.

Figure 4. Station hall floor model plan.

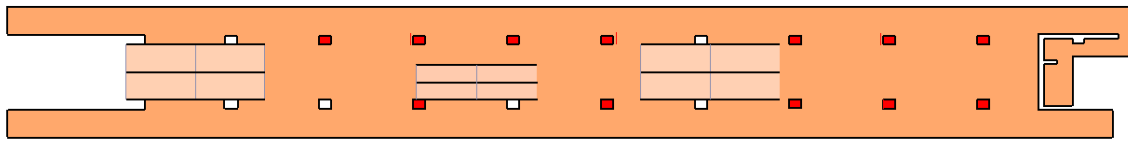**Figure 5.** Model plan of platform 2.
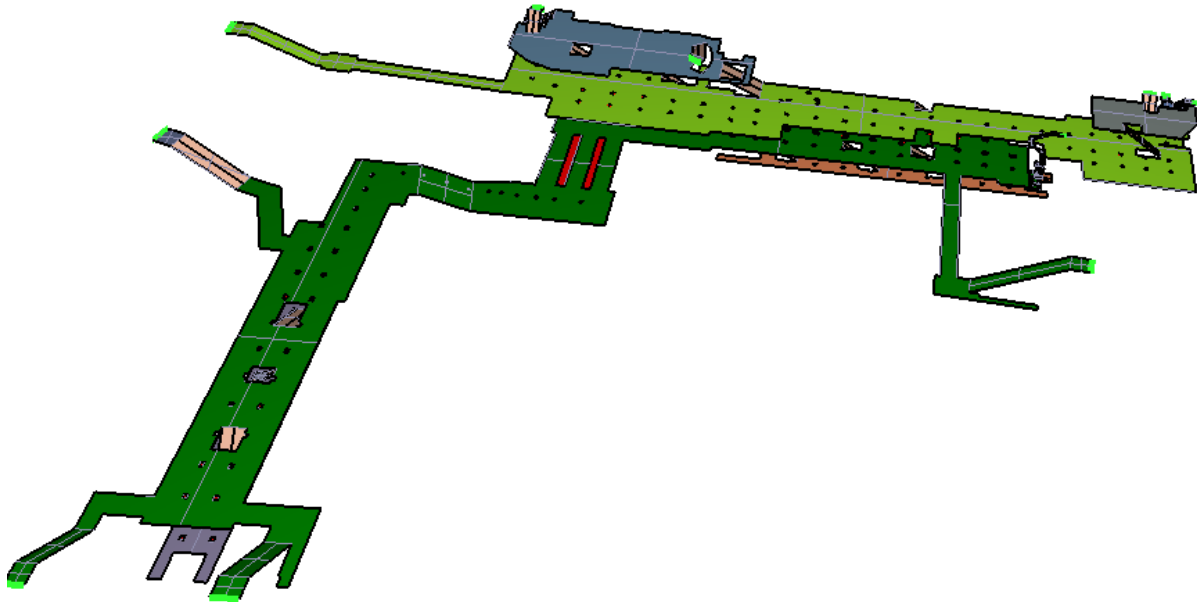
Figure 6. Model plan of platform 5.

Figure 7. Schematic diagram of the overall 3D model.

2.2. Construction of Pedestrian Number and Speed Factor Based on Monte Carlo

The determination of constraint parameters mainly includes the determination of the number of evacuated pedestrians and indicators of evacuated pedestrians.

(1) According to the area of each region of the model, the pedestrian density range is set to 0.5~4.5 m^2/person. By setting a larger range of pedestrian density and expanding the range of evacuated pedestrians, the applicability and correctness of the model are improved. The specific parameters can be determined according to the specific conditions of the city and the station. Assuming that the pedestrian density is 1.5 m^2/person, the total number of pedestrians involved in the evacuation is 20,731.4/1.5 = 13,821.

(2) During the evacuation process, the number and walking speed of various groups of pedestrians will affect the evacuation time. From the count of the number of pedestrians of different ages taking the subway in literature [31], it can be seen that the subway pedestrian is mainly young and middle-aged, and about 86.6% are between 18 and 60 years old. Crowds aged 18 and below and over 60 accounted for a relatively small proportion of 6.6% and 6.8%, respectively. It is known that the normal walking speed of pedestrian walking is generally 5 km/h = 1.38 m/s [32], and this walking speed is changed according to the age of the pedestrian. For example, the walking speed of an adult is generally faster than that of a child and the elder, and the walking speed of a child is generally faster than that of the elder. Taking the reduction coefficients as 1, 0.8, and 0.75 [31], respectively, the basic walking speeds of the three groups of pedestrians are calculated to be 1.38 m/s, 1.10 m/s, and 1.035 m/s, respectively.

In addition, the normal distribution is used for the setting when establishing the simulated character model. For example, the adult height range is set to 1.55 m~1.85 m, the average is 1.73 m, and the standard deviation is 0.05 m. The specific parameter distribution of each population is shown in Tables 1 and 2.

Table 1. The height parameters of the simulated pedestrian.

Pedestrian Group	Distribution	Min (m)	Max (m)	Average (m)	Standard Deviation (m)
Adult	Normal distribution	1.55	1.85	1.73	0.05
Child	Normal distribution	1.0	1.6	1.4	0.05
Elder	Normal distribution	1.5	1.75	1.61	0.05

Table 2. The shoulder width parameters of the simulated pedestrian.

| Pedestrian Group	Distribution	Min (m)	Max (m)	Average (m)	Standard Deviation (m)
Adult	Normal distribution	0.42	0.55	0.48	0.03
Child	Normal distribution	0.34	0.48	0.38	0.03
Elder	Normal distribution	0.39	0.51	0.44	0.03

The Monte Carlo method was used to randomly select 30 sample parameters in the density range of 0.5~4.5 (m²/person). The training model is more feasible by setting a larger range of pedestrian's density to expand the range of evacuated pedestrians. For the walking speed, in the event of a disaster, it should be taken into account that some pedestrians are running at a faster pace or that some injured pedestrians are walking slower than normal. Therefore, the basic walking speed of each group is multiplied by the speed factor, and the coefficient range is between 0.5 and 3. Setting a larger speed factor range can meet the fast or slow walking speeds of pedestrians in different states. In total, 30 groups of data parameters were input and simulated, and the simulated parameters and evacuation time of each group are shown in Table 3.

Table 3. Sample data and escape time randomly selected based on the Monte Carlo method.

Case	Space Occupation (m²/pers)	Density (pers/m²)	Speed Factor	Number of Pedestrians (per)	Evacuation Time (s)
1	0.844	1.185	1.241	24,567	897.6
2	3.704	0.270	0.972	5597	410
3	4.216	0.237	0.959	4913	396.9
4	2.456	0.407	2.064	8438	279.9
5	1.448	0.691	0.703	14,325	1006.8
6	4.352	0.230	2.439	4768	152.3
7	1.694	0.509	2.323	12,240	286.4
8	3.760	0.266	1.266	5515	307.3
9	3.216	0.311	1.777	6447	274.6
10	1.968	0.508	2.487	10,532	280.2
11	0.652	1.534	1.447	31,802	870.1
12	4.152	0.241	1.832	4996	222.6
13	1.876	0.533	2.594	11,053	271.9
14	1.563	0.640	2.167	13,266	327.6
15	1.048	0.954	1.968	19,778	456.3
16	0.928	1.078	1.253	22,348	753.4
17	2.476	0.404	1.076	8375	491.5
18	3.360	0.298	0.987	6178	439.7
19	4.416	0.226	1.297	4685	295.9
20	3.296	0.303	1.589	6282	281.1
21	0.624	1.603	2.808	33,232	480
22	2.500	0.400	0.962	8293	560.8
23	4.120	0.243	2.949	5033	134
24	2.972	0.336	0.778	6966	623.7
25	3.720	0.269	1.522	5577	274
26	1.232	0.812	1.156	16,834	668.1
27	4.048	0.247	2.278	5121	201.3
28	3.028	0.330	0.794	6833	563.3
29	4.064	0.246	0.927	5100	400.6
30	0.740	1.351	1.770	28,008	648

Table 3 shows that among the 30 sets of randomly generated data, only 14 sets of samples meet the required safe evacuation time and can achieve safe escape for all pedestrians.

The rest of the sample data evacuation time is greater than 330 s, and the evacuation time of some samples is far more than 330 s, which means there is a huge security risk. The mapping relationship between the speed factor, the number of pedestrians evacuated, and the evacuation time is shown in Figure 8. It shows a relatively flat mapping curve for the speed factor, the number of pedestrians evacuated, and the evacuation time. When the number of pedestrians increases or the speed factor increases, the evacuation time will show a linear-plane growth or attenuation.
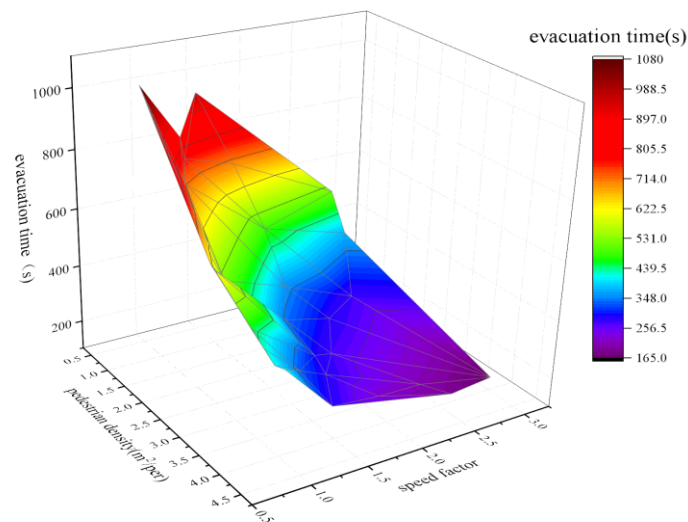
Figure 8. The relationship between speed factor, number of evacuees, and evacuation time.

2.3. Introduction to the Principle of Support Vector Machine

The support vector machine (SVM) is a mathematical method that can perform binary classification according to data characteristics and is a linear classifier with the largest interval defined in the feature space. The core idea is to divide the separation hyperplane with the largest geometric distance of different types of data according to the data samples, as shown in Figure 9.
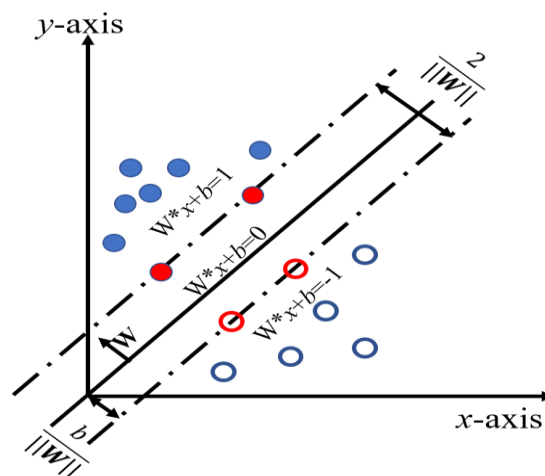
Figure 9. SVM schematic.

The blue circles in Figure 9 represent data points. Solid circles are classified as one type of data and hollow ones as another. The red circle is used as an important sample for classification.

3. Result Analysis

### 3.1. Analysis of Pedestrian Escape Time and Number in Each Sample

In order to further understand the changes in the number of pedestrians evacuated over time, according to the range of the number of random samples, the samples of 0–10,000, 10,000–20,000, and 20,000–30,000 pedestrians were divided into three groups, respectively. The specific grouping situation is shown in Table 4, and the relationship curve between the number of pedestrians who failed to escape and time is drawn, as shown in Figures 10–12.
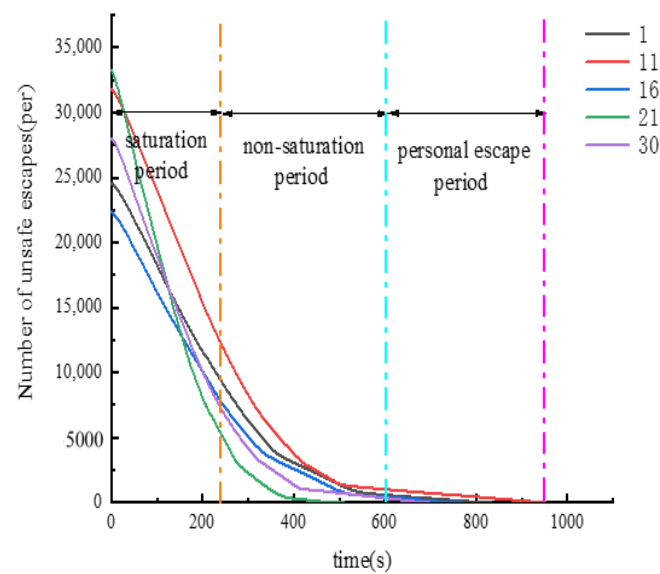
Table 4. Sample groupings.

Number of Pedestrians	Group	Sample Serial Number
0~10,000	A	2, 3, 4, 6, 8, 9, 12, 17, 18, 19, 20, 22, 23, 24, 25, 27, 28, 29
10,000~20,000	B	5, 7, 10, 13, 14, 15, 26
More than 20,000	C	1, 11, 16, 21, 30
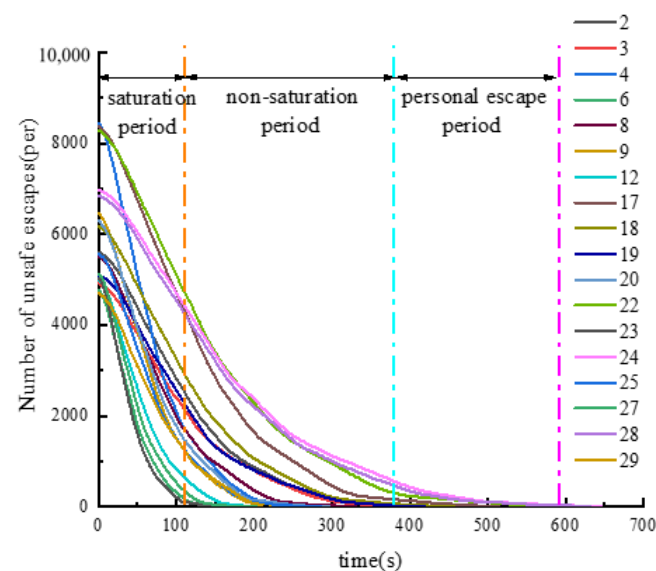
Figure 10. The curve of the number of pedestrians who failed to escape in group A with time.
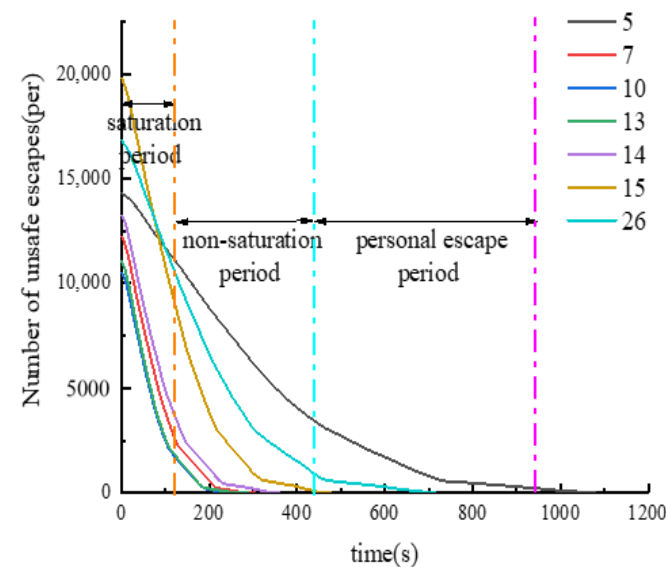

Figure 11. The curve of the number of pedestrians who failed to escape in group B with time.

Figure 12. The curve of the number of pedestrians who failed to escape in group C with time.

Figures 10–12 show that all the curves basically show a concave change; that is, with the increase of time, the number of pedestrians fleeing the subway station per unit of time is gradually decreasing. A 3D visualization of the escape was performed (Figure 13). According to the changing form of the curve, pedestrian escape is divided into three periods: saturation period, non-saturation period, and personal escape. For example, within 0~110 s (saturation period) of the samples in group A, all the curves basically decline linearly, and the flow of the pedestrian at all exits in the subway reaches the maximum value at this time. The exit of the passage is in a saturated state, and a large number of pedestrians gather at the exit to escape (Figure 14a), resulting in congestion. Within 110~380 s (half-saturation period), the slope of the curve decreases. At this time, the pedestrian flow at each exit is relatively small (Figure 14b), and some exits have even been idle, and no one has passed. Within 380~590 s (personal escape period), the evacuation of pedestrians in the subway has basically been completed, and only a few pedestrians who are injured or have a slow walking speed are left to escape slowly.


(**a**)　　　　　　　　　　　　　　　　　　　　　(**b**)
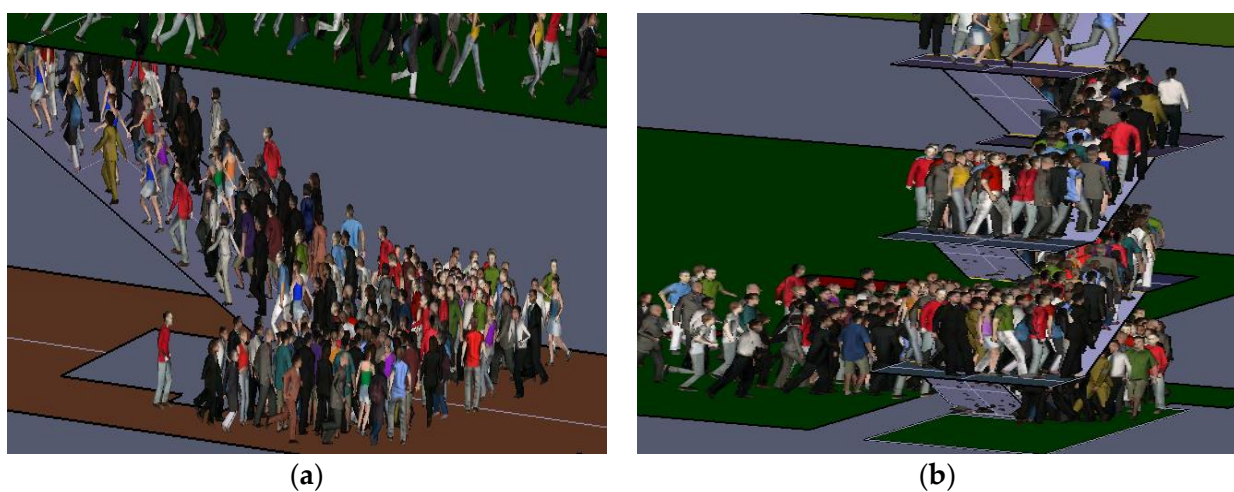
Figure 13. (**a**) Evacuation in platform 5; (**b**) Evacuation in Station hall floor.

(a)

(b)
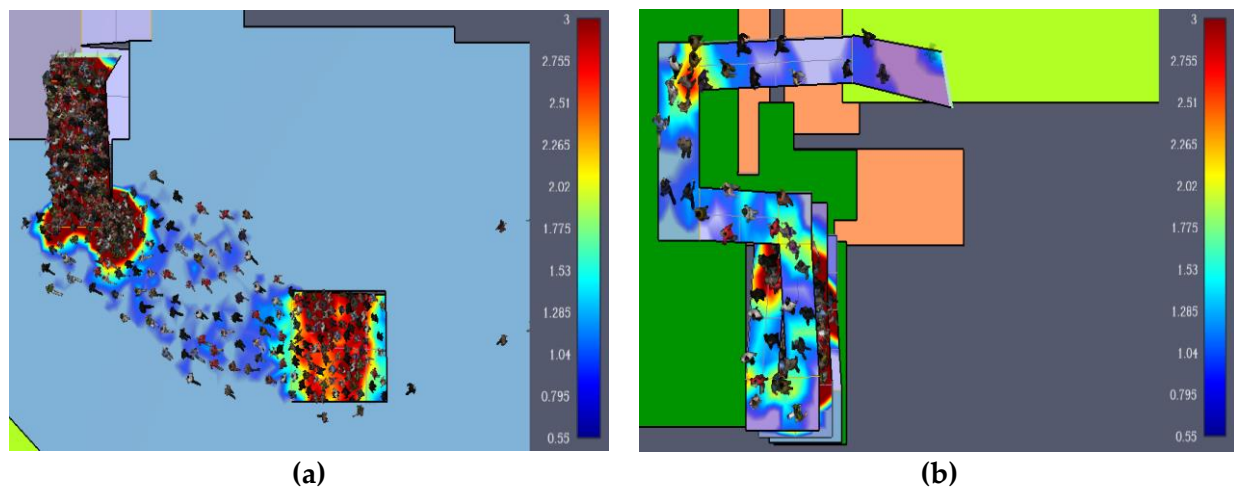
Figure 14. (**a**) Density of export pedestrians during saturation period; (**b**) Density of export pedestrians in unsaturated period.

3.2. Analysis of Pedestrian Passage Time and Number at Different Exits

Figures 10–12 show that the upper limit of escape time is determined by the walking speed of the pedestrian. For example, the total number of pedestrians in sample 5 in Figure 11 is 14,325, and the total escape time is as long as 1006.8 s, far exceeding the same group of samples. The single-person escape time accounts for more than half of the total time. The fundamental reason is that the walking speed is too slow. When pedestrians are distributed far from the safe passage, the time cost will increase significantly. In addition, due to the slower walking speed, the decreasing slope of the variation curve of sample 5 during the saturation period is also much lower than that of the same group. Although a slower walking speed can reduce stampede incidents caused by crowds, it will also greatly improve the safe evacuation time of all pedestrians. In order to further understand the pedestrian evacuation in the unsaturated period, samples 23 and 28 were randomly selected as examples to analyze the specific conditions of the 12 exits in the subway station during a safe evacuation, as shown in Figures 15 and 16.
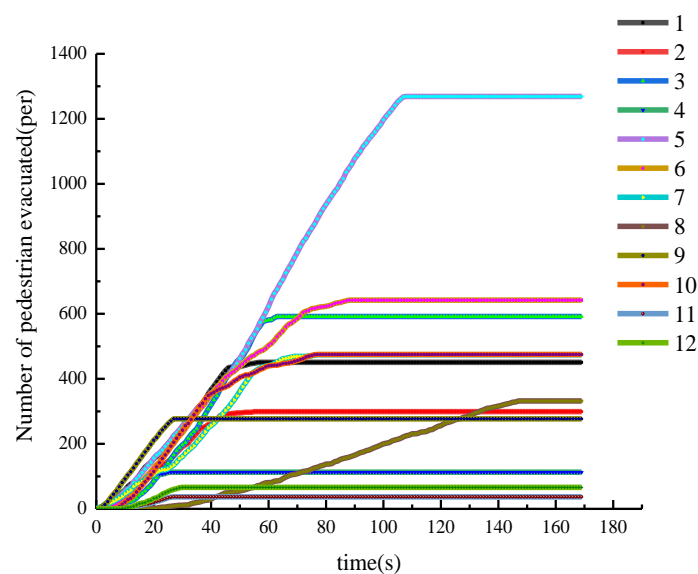
Figure 15. Number of pedestrians passing through each exit and travel time of sample 23.
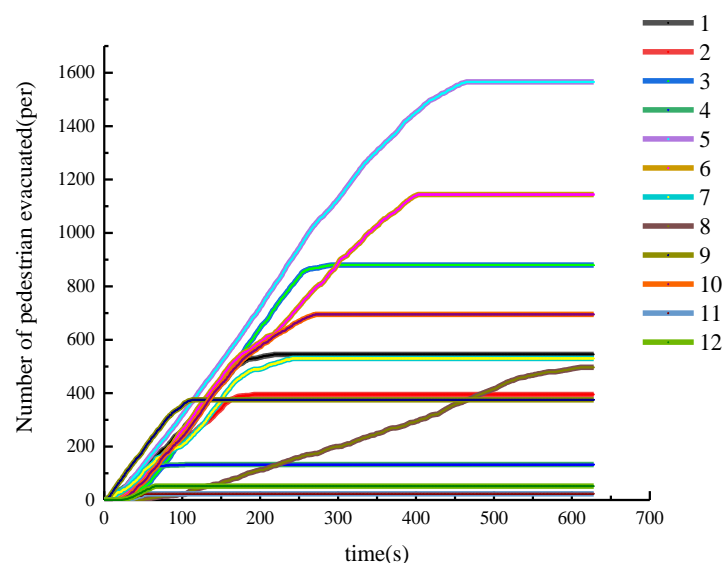
Figure 16. Number of pedestrians passing through each exit and travel time of sample 28.

Figure 15 shows the evacuation of pedestrians from all exits in sample 23. The total evacuation time for this simulation is 563 s. Exit 5 has the largest number of escapees, and the maximum flow of pedestrians exceeds seven pedestrians. A total of 1592 pedestrians pass through, accounting for 23.3% of the total number of pedestrians. It is the most important exit in this evacuation process. In addition, it can be seen that all exits in the early evacuation period (0~50 s) were fully utilized. With the advancement of time, Exits 4, 9, 11, and 12 have been unmanned within 50 to 110 s, and these exits will be idle in subsequent moments, and no one will pass. Exits 1, 2, 3, 7, and 10 end at 110~260 s, Exits 5 and 6 end at 400~450 s, and Exit 8 (530~540) is the last exit of this evacuation simulation work.

For comparison only from working hours, Exit 8 is about four times that of Exits 4, 9, 11, and 12, but the number of pedestrians is much lower than that of Exit 5. This result is because Exit 8 is an emergency escape exit, and the stairwell of exit 8 is narrower than other exits. During the evacuation process, the maximum flow of pedestrians at Exit 8 was only two pedestrian/s, while the peak flow of pedestrians at the other exits was greater than seven pedestrian/s. Pedestrian herd behavior leads to serious uneven distribution of evacuation resources, and the narrow stairwells and congestion greatly prolong the safe escape time of pedestrians.

The evacuation curves of sample 23 (Figure 15) and sample 28 (Figure 16) were compared, and their overall trend was almost the same. Among them, Exits 5 and 6 are the most important exits for evacuation, and they basically undertake 40% of the evacuation of pedestrians. They are very important exits, and the smooth flow of these two exits should be ensured at all times. In addition, the evacuation guidance of Exits 4, 9, 11, and 12 should be strengthened so as to prolong the passage time of the four exits. Reasonable allocation of evacuation resources to ensure the maximum efficiency of evacuation. The specific parameters of the number of pedestrians passing through each exit of samples 23 and 28 and the passage time are shown in Tables 5 and 6.

3.3. Calculation of Minimum Pedestrian Escape Speed Based on SVM

The above analysis shows that the number of pedestrians and walking speed are important factors affecting the overall evacuation time. In order to further study the internal criteria of whether pedestrians can escape safely during the evacuation, a support vector machine (SVM) [33] is introduced for data analysis.

The data in Tables 3 and 7 are brought into the SVM theory, the number of pedestrians evacuated and the walking speed factor are used as sample indicators, and the 330 s escape time in the safety specification is used as the critical time point. The escape time is

greater than or equal to 330 s, which means that the escape failed. Otherwise, the escape is successful. See Table 7 for all the statistics.

Table 5. Number of pedestrians evacuated and evacuation time at each exit of sample 23.

Exit	Number of Pedestrians (per)	Proportion (%)	Evacuation Time (s)
1	448	8.90	51
2	309	6.14	50
3	586	11.64	59
4	112	2.23	26
5	1292	25.67	105
6	658	13.07	88
7	441	8.76	68
8	307	6.10	135
9	271	5.38	27
10	502	9.98	76
11	39	0.78	29
12	68	1.35	32

Table 6. Number of pedestrians evacuated and evacuation time at each exit of sample 28.

Exit	Number of Pedestrians (per)	Proportion (%)	Evacuation Time (s)
1	544	7.97	202
2	399	5.84	165
3	885	12.95	259
4	133	1.95	79
5	1592	23.30	450
6	1109	16.23	404
7	536	7.84	206
8	484	7.08	536
9	375	5.49	108
10	701	10.26	259
11	23	0.33	51
12	52	0.76	66

Table 7. Classification of escape results in each sample.

	Escape Result	Sample Serial Number
Failed to escape (time $\leq$ 330)	Success	4, 6,7, 8, 9, 10, 12, 13,14, 19 20, 23, 25, 27
Escape success (time > 330)	Fail	1, 2, 3, 5, 11, 15, 16, 17, 18, 21, 22, 24, 26, 28, 29, 30

The first 20 groups of samples are used as the training data, and the last 10 groups are used as the test data (only the index data is included in the test data, and the actual data is not included). The available classification result graph is shown in Figure 17, and the classification result data is shown in Table 6. The final classification hyperplane result equation is solved as follows:

$$y - 0.6762 \times 10^{-4}x - 0.8828 = 0 \ (x > 0) \tag{1}$$

Among them, y represents the speed factor, and x represents the number of pedestrians. For evacuation simulations with different numbers of pedestrians and walking speed coefficients, if the result is greater than or equal to 0 after it is brought into formula (1), it is determined that the escape is successful, and all pedestrians in the subway can escape safely. If the result is less than 0, it is determined that the escape failed, the subway pedestrians cannot achieve all safe escape.

Table 8 and Figure 17 show the classification results of this SVM, and the training samples simulated by this classification are all correctly divided. For the predicted samples, comparing the actual classification results in Table 8, it can be seen that the predicted results are completely correct, and the prediction accuracy is 100%. Therefore, it can be considered that the separation hyperplane equation of this SVM is accurate and effective. That is, by inputting the number of pedestrians in the subway and the walking speed of the pedestrians, it can be determined whether all the pedestrians in the subway can escape within the safety specification time by relying on the Formula (1).
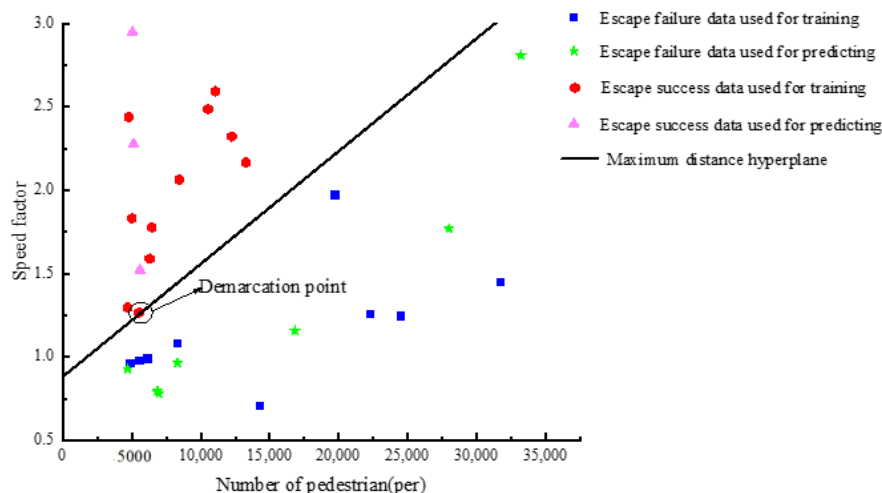

Figure 17. SVM classification results.

Table 8. Comparison of test classification results and SVM classification results.

Sample Serial Number	Simulation Results	SVM Classification Results
21	Fail	Fail
22	Fail	Fail
23	Success	Success
24	Fail	Fail
25	Success	Success
26	Fail	Fail
27	Success	Success
28	Fail	Fail
29	Fail	Fail
30	Fail	Fail

Observing Formula (1), we can see that when $x = 1$, y is almost equal to 0.8828. The physical meaning of this result is: When there is only one person in the subway station, and the position of the person satisfies the random distribution, then the minimum walking speed to ensure that he can escape successfully is 0.8828×1.035 m/s (the walking speed of the old man) = 0.9137 m/s.

In this paper, the basic pedestrian speed is set as 5 km/h. By setting the speed coefficient of 0.5~3, the actual range of pedestrian moving speed will be expanded to 0.52 m/s (1.035 m/s × 0.5)~4.14 m/s (1.38 ms × 3), and the minimum escape speed can be solved in this range. The basic speed of the pedestrian itself is not critical because the speed factor will make the speed range of the pedestrian include the minimum escape speed, and then the SVM can be solved. For example, set the pedestrian's base speed to be 1 m/s and the actual escape speed is 0.9 m/s, then the speed factor calculated by the SVM is 0.9. Set the pedestrian base speed to 0.5 m/s, and the actual escape speed is 0.9 m/s, then the velocity coefficient calculated by SVM is 1.8. Therefore, the basic speed of pedestrians is not critical. As long as the speed range includes the minimum escape speed, the speed factor

will change accordingly, and the final calculated minimum escape speed will be basically the same.

Taking the escape situation of normal pedestrians as an example, assuming that the walking speed factor is set to 1.5. That is, the pedestrians in the subway station escape at a walking speed of 1.5 times the usual walking speed, then the Formula (1) shows that the maximum number of pedestrians carrying the Nanning Mingxiu Road Station is:

$$x = \frac{1.5 - 0.8828}{0.6762 \times 10^{-4}} = 9127 \ (\text{per}) \tag{2}$$

In daily traffic, the number of pedestrians in the Mingxiu Road station should be less than 9127 to ensure the safe evacuation of all pedestrians in an emergency. In case of heavy rain or other extreme weather, the walking speed of pedestrians should be smaller, and the specific walking speed should be analyzed according to the actual situation.

3.4. Calculation of Critical Water Level Height Based on Minimum Escape Speed

In Section 3.3, the SVM model was used to solve the minimum escape speed of pedestrians as 0.914 m/s. However, there will be a flood in the subway station due to a rainstorm (Figure 18), and when the flood height exceeds the critical value, the resistance and buoyancy brought by the flood will make people unable to reach the minimum escape speed of 0.914 m/s, resulting in the failure of escape.
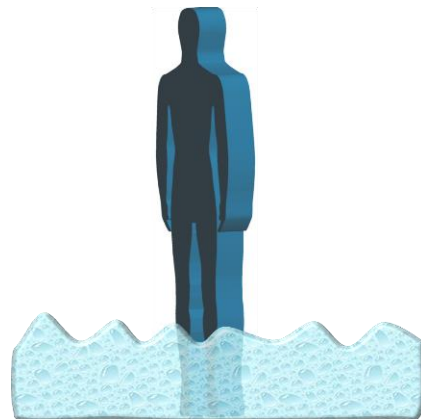

**Figure 18.** A sketch of a model of a man in a flood.

Therefore, when the flood height exceeds the critical value, the walking speed of pedestrians will not reach 0.914 m/s, so the escape will fail. In order to accurately solve the critical value of the height of the flood, a 1:1 contour height model was constructed for all groups (adult, child, elder). The model height was consistent with the simulated height in Section 3 (adult = 173 cm, child = 140 cm, and the elder = 161 cm). The flood height is set to 10 cm, 20 cm, 30 cm, 40 cm, 50 cm, 60 cm, 70 cm, 80 cm, 90 cm, and 100 cm. Since pedestrians keep relative movement with the flood when moving, the pedestrian velocity = 0.914 m/s and the flood velocity = 0 m/s can be converted to the flood velocity = 0.914 m/s and the pedestrian velocity = 0 m/s so as to simulate the impact resistance of flood flow to pedestrians at different flood heights. Dynamic flood pressure of all groups is shown in Figures 19–21, and dynamic flood resistance is shown in Table 9.
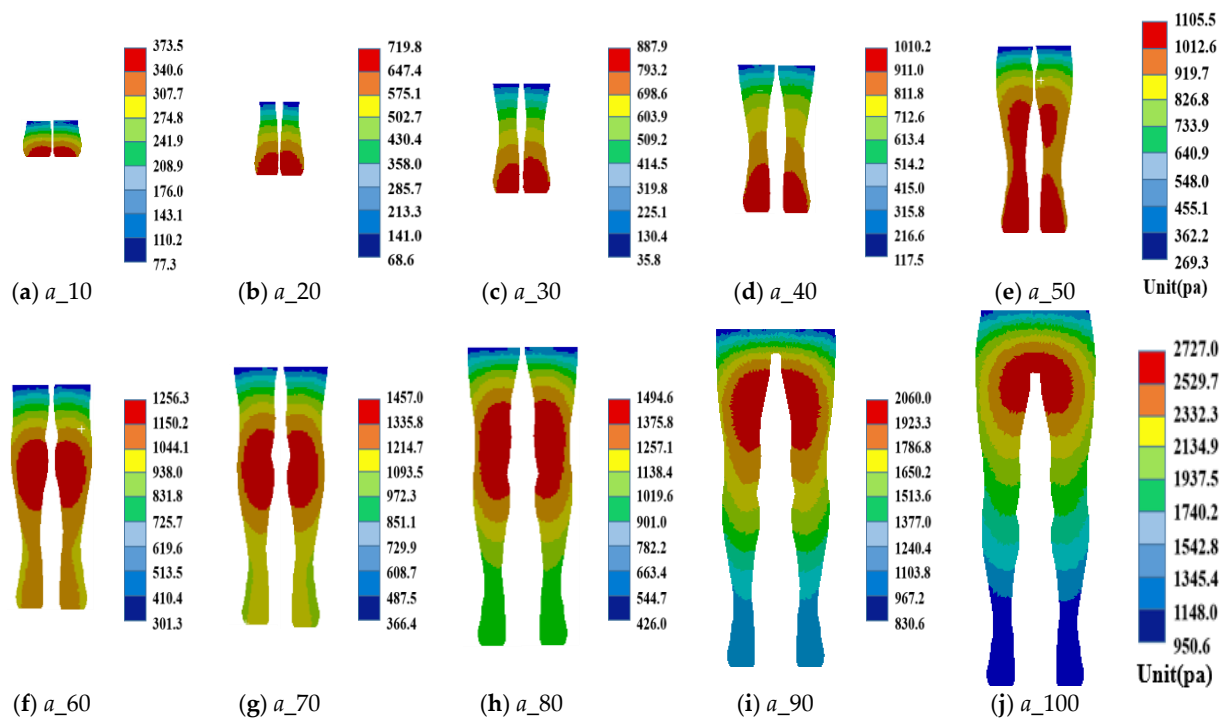
Figure 19. Hydrodynamic pressure of adult walking at a minimum safe speed at different flood heights.
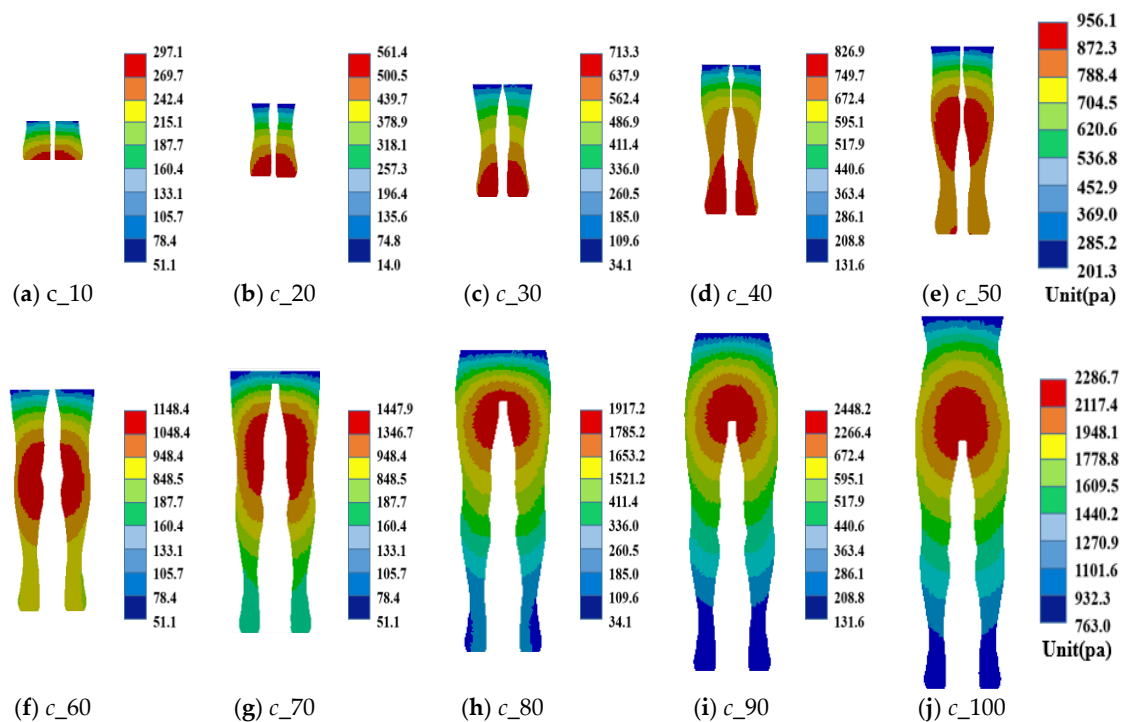
Figure 20. Hydrodynamic pressure of child walking at a minimum safe speed at different flood heights.
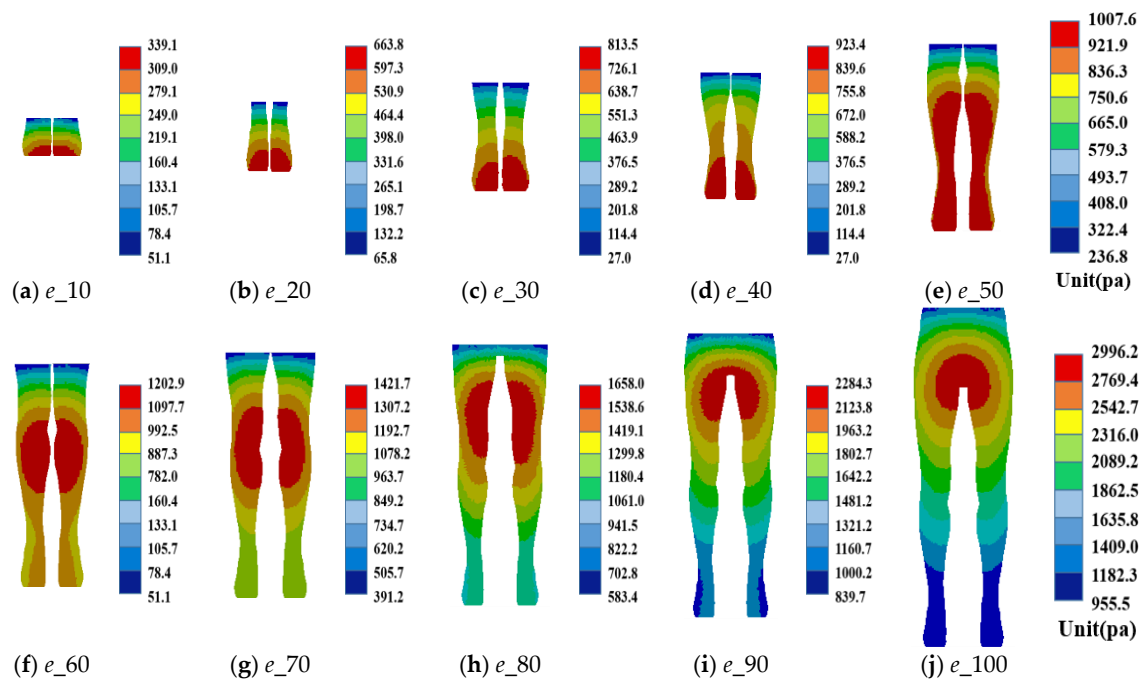
Figure 21. Hydrodynamic pressure of elder walking at a minimum safe speed at different flood heights.

Table 9. Flood resistance of all groups walking at a critical speed at different flood heights.

Flood Height (cm)	Adult	Child	Elder
10	3.6 N	2.0 N	2.9 N
20	6.4 N	6.7 N	9.7 N
30	21.6 N	15.3 N	18.8 N
40	40.9 N	30.8 N	36.6 N
50	67.9 N	48.4 N	59.8 N
60	94.9 N	73.9 N	86.3 N
70	116.5 N	116.4 N	124.2 N
80	162.3 N	175.8 N	172.7 N
90	261.3 N	252.0 N	269.0 N
100	372.2	275.6	386.2

The calculation formula of friction between pedestrians and the ground in flood is as follows:

$$F = f \times (Mg - W) \tag{3}$$

F represents the friction between the pedestrian and the ground, f represents the friction factor between the pedestrian and the ground, M represents the mass of the pedestrian, g represents the acceleration of gravity ($9.8 \, \text{m/s}^2$), W represents the buoyancy of the pedestrian in flood, and the specific expression of buoyancy W is:

$$W = \rho g V \tag{4}$$

ρ represents the density of the liquid, and V represents the volume of the flood displaced by the pedestrian standing in it (Table 10). As for M, the simplified BMI index of 21.5 [34] was used as the calculation. Based on the average height in Section 3, the standard weight of each group was calculated as follows: adult = 64.3 kg, child = 42.2 kg, and the elder = 55.7 kg.

$$\text{BMI} = \frac{M}{H^2} \tag{5}$$

**Table 10.** The drainage volume of all groups in flood at different flood heights.

| Flood Height (cm)	Adult	Child	Elder
10	0.00136 m^3	0.00106 m^3	0.00124 m^3
20	0.0024 m^3	0.0019 m^3	0.0022 m^3
30	0.0036 m^3	0.0031 m^3	0.0034 m^3
40	0.0054 m^3	0.0047 m^3	0.0051 m^3
50	0.0073 m^3	0.0062 m^3	0.0069 m^3
60	0.0092 m^3	0.0080 m^3	0.0087 m^3
70	0.0113 m^3	0.0104 m^3	0.0109 m^3
80	0.014 m^3	0.0128 m^3	0.0136 m^3
90	0.017 m^3	0.0150 m^3	0.0164 m^3
100	0.02 m^3	0.0170 m^3	0.0190 m^3

BMI stands for pedestrian mass index, *H* is the height of the pedestrian, *M* is the mass of the pedestrian.

The drainage volume data in Table 10, adults = 64.3 kg, children = 42.2 kg, elderly = 55.7 kg, g = 9.8 m/s^2, ρ = 1000 kg/m3, f = 0.5 [35], are substituted into Equations (3) and (4). The friction force between the pedestrian and the ground at different flood heights is calculated and compared with the flood resistance of the pedestrian. Table 11 shows the comparison results, and Figures 22–24 show the comparison curve.

Table 11. Friction and flood resistance of all groups when walking at a critical speed at different flood heights.

Flood Height (cm)	Adult		Child		Elder	
	Friction	Flood Resistance	Friction	Flood Resistance	Friction	Flood Resistance
10	308.4	3.6	201.5	2.0	266.8	2.9
20	303.3	6.4	197.4	6.7	262.1	9.7
30	297.4	21.6	191.5	15.3	256.2	18.8
40	288.6	40.9	183.7	30.8	247.9	36.6
50	279.3	67.9	176.4	48.4	239.1	59.8
60	269.9	94.9	167.5	73.9	230.3	86.3
70	259.7	116.5	155.8	116.4	219.5	124.2
80	246.4	162.3	144.0	175.8	206.2	172.7
90	231.7	261.3	133.2	252.0	192.5	269.0
100	217.0	372.2	123.4	275.6	179.8	386.2
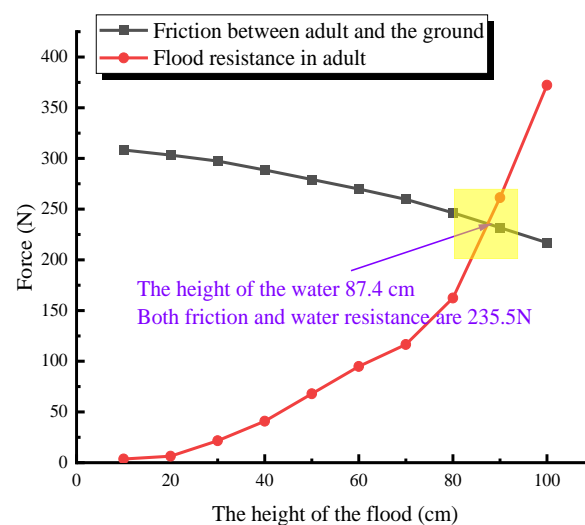
Figure 22. Curve comparison of the flood resistance and friction (adult).
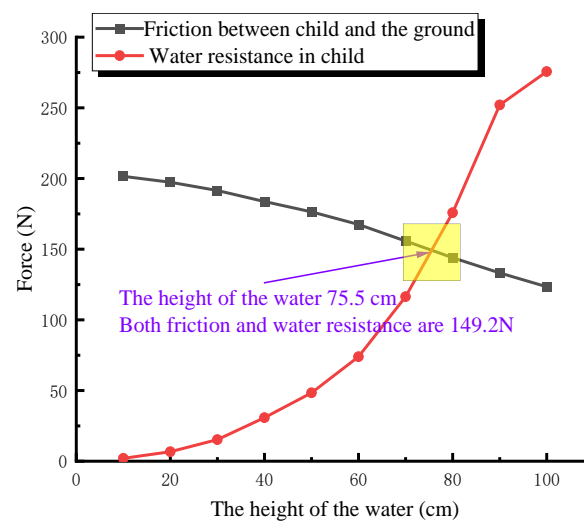
Figure 23. Curve comparison of the flood resistance and friction (child).
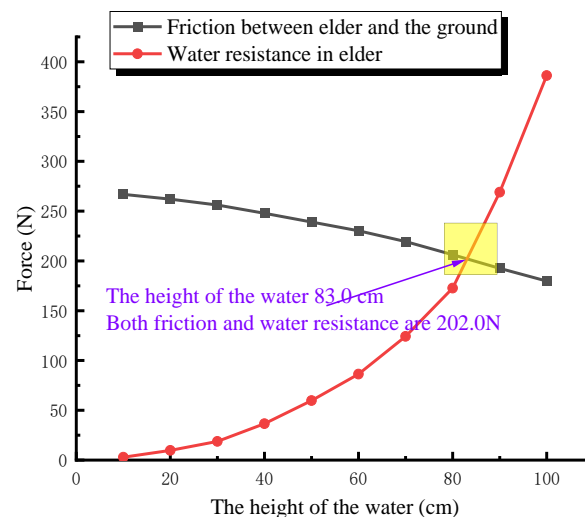
Figure 24. Curve comparison of the flood resistance and friction (elder).

The intersection of curves in Figures 22–24 was calculated, and the critical flood heights for adults, children, and the elder to escape were 87.4 cm, 75.5 cm, and 83.0 cm, respectively. For an adult, when the height of the flood in the subway is greater than 87.4 cm, the walking speed of adults cannot reach 0.914 m/s, so the safety escape cannot be completed within the specified 330 s.

4. Conclusions

(1) Based on the model of the Mingxiu Road subway station in Nanning city, China, the maximum daily pedestrian capacity of the Mingxiu Road subway station is calculated to be 9127 using the Monte Carlo, 3D simulation, and SVM methods. The minimum speed of pedestrian safety escape is 0.914 m/s.

(2) The minimum escape speed was 0.914 m/s as the critical speed. Set different flood heights and compare the flood resistance and friction between pedestrians and the ground. Finally, the critical escape flood level heights of adults, children, and the elderly are 87.4 cm, 75.5 cm, and 83.0 cm, respectively.

References

1. Wang, H.-B.; Gong, X.-S.; Wang, B.-B.; Deng, C.; Cao, Q. Urban development analysis using built-up area maps based on multiple high-resolution satellite data. *Int. J. Appl. Earth Obs. Geoinf.* **2021**, *103*, 1102500. [CrossRef]
2. Li, X.-y.; Lu, Z.-h. Quantitative measurement on urbanization development level in urban Agglomerations: A case of JJJ urban agglomeration. *Ecol. Indic.* **2021**, *133*, 108375. [CrossRef]
3. Liu, B.; Lin, H.; Chen, Y.; Liu, J.; Guo, C. Deformation Stability Response of Adjacent Subway Tunnels considering Excavation and Support of Foundation Pit. *Lithosphere* **2022**, *2022*, 7227330. [CrossRef]
4. Löwe, R.; Mair, M.; Pedersen, A.N.; Kleidorfer, M.; Rauch, W.; Arnbjerg-Nielsen, K. Impacts of urban development on urban water management—Limits of predictability. *Comput. Environ. Urban Syst.* **2020**, *84*, 101546. [CrossRef]
5. Wang, H.; Qin, F.; Xu, C.; Li, B.; Guo, L.; Wang, Z. Evaluating the suitability of urban development land with a Geodetector. *Ecol. Indic.* **2021**, *123*, 1–13. [CrossRef]
6. Herrmann, C.R.; Maroko, A.R.; Taniguchi, T.A. Subway Station Closures and Robbery Hot Spots in New York City-Understanding Mobility Factors and Crime Reduction. *Eur. J. Crim. Policy Res.* **2021**, *27*, 415–432. [CrossRef]
7. Cui, J.; Broere, W.; Lin, D. Underground space utilisation for urban renewal. *Tunn. Undergr. Space Technol.* **2021**, *108*, 103726. [CrossRef]
8. Zhang, Y.-H.; Zhu, J.-B.; Liao, Z.-Y.; Guo, J.; Xie, H.-P.; Peng, Q. An intelligent planning model for the development and utilization of urban underground space with an application to the Luohu District in Shenzhen. *Tunn. Undergr. Space Technol.* **2021**, *112*, 103933. [CrossRef]
9. Xu, W.; Liu, B.; Liu, J.; Guo, C. Interactions of Foundation Pit on the Underlying Adjacent Existing Underground Structures. *Geofluids* **2022**, *2022*, 5675173. [CrossRef]
10. Liu, S.-C.; Peng, F.-L.; Qiao, Y.-K.; Zhang, J.-B. Evaluating disaster prevention benefits of underground space from the perspective of urban resilience. *Int. J. Disaster Risk Reduct.* **2021**, *58*, 102206. [CrossRef]
11. Han, G.; Leng, J.-W. Urban underground space planning based on FPGA and virtual reality system. *Microprocess. Microsyst.* **2021**, *80*, 103601. [CrossRef]
12. Gonzalez-Navarro, M.; Turner, M.A. Subways and urban growth: Evidence from earth. *J. Urban Econ.* **2018**, *108*, 85–106. [CrossRef]
13. Dou, F.-F.; Li, X.-H.; Xing, H.-X.; Yuan, F.; Ge, W.-Y. 3D geological suitability evaluation for urban underground space development—A case study of Qianjiang Newtown in Hangzhou, Eastern China. *Tunn. Undergr. Space Technol.* **2021**, *115*, 104052. [CrossRef]
14. Tan, F.; Wang, J.; Jiao, Y.-Y.; Ma, B.-C.; He, L.-L. Suitability evaluation of underground space based on finite interval cloud model and genetic algorithm combination weighting. *Tunn. Undergr. Space Technol.* **2021**, *108*, 103743. [CrossRef]
15. Yoon, Y.K. Usability Test for Mobile Subway Application. *J. Cult. Prod. Des.* **2018**, *53*, 89–97. [CrossRef]
16. van der Wal, C.N.; Robinson, M.A.; de Bruin, W.B.; Gwynne, S. Evacuation behaviors and emergency communications: An analysis of real-world incident videos. *Saf. Sci.* **2021**, *136*, 105121. [CrossRef]
17. Cheng, H.; Yang, X.-K. Emergency Evacuation Capacity of Subway Stations. *Procedia Soc. Behav. Sci.* **2012**, *43*, 339–348. [CrossRef]
18. Zhou, M.; Ge, S.-C.; Liu, J.-L.; Dong, H.-R.; Wang, F.-Y. Field observation and analysis of waiting passengers at subway platform—A case study of Beijing subway stations. *Phys. A Stat. Mech. Its Appl.* **2020**, *556*, 124779. [CrossRef]

19. Lyu, H.-M.; Shen, S.-L.; Zhou, A.-N.; Yang, J. Perspectives for flood risk assessment and management for mega-city metro system. *Tunn. Undergr. Space Technol.* **2019**, *84*, 31–44. [CrossRef]

20. Lyu, H.-M.; Shen, S.-L.; Zhou, A.-N.; Zhou, W.-H. Flood risk assessment of metro systems in a subsiding environment using the interval FAHP-FCA approach. *Sustain. Cities Soc.* **2019**, *50*, 101682. [CrossRef]

21. Qu, Y.-C.; Gao, Z.-Y.; Xiao, Y.; Li, X.-G. Modeling the pedestrian's movement and simulating evacuation dynamics on stairs. *Saf. Sci.* **2014**, *70*, 189–201. [CrossRef]

22. Wang, J.-H.; Yan, W.-Y.; Zhi, Y.-R.; Jiang, J.-C. Investigation of the Panic Psychology and Behaviors of Evacuation Crowds in Subway Emergencies. *Procedia Eng.* **2016**, *135*, 128–137. [CrossRef]

23. Yi, J.-X.; Pan, S.-L.; Chen, Q. Simulation of pedestrian evacuation in stampedes based on a cellular automaton model. *Simul. Model. Pract. Theory* **2020**, *104*, 102147. [CrossRef]

24. Feng, J.-R.; Gai, W.-M.; Yan, Y.-B. Emergency evacuation risk assessment and mitigation strategy for a toxic gas leak in an underground space: The case of a subway station in Guangzhou, China. *Saf. Sci.* **2021**, *134*, 105039. [CrossRef]

25. Ying, Z.; Xin-Gang, L.; Bin, J.; Rui, J. Simulation of pedestrians' evacuation dynamics with underground flood spreading based on cellular automaton. *Simul. Model. Pract. Theory* **2019**, *94*, 149–161.

26. Yukawa, S.; Hatayama, M.; Tatano, H. A study of evaluation method for large-scale flood evacuation planning using the network equilibrium analysis. *J. Jpn. Soc. Civ. Eng. Ser D3* **2011**, *67*, 177–188.

27. Uno, K.; Kashiyama, K. Development of Simulation System for the Disaster Evacuation Based on Multi-Agent Model Using GIS. *Tsinghua Sci. Technol.* **2008**, *13*, 348–353. [CrossRef]

28. Simonovic, S.P.; Ahmad, S. Computer-based Model for Flood Evacuation Emergency Planning. *Nat. Hazards* **2005**, *34*, 25–31. [CrossRef]

29. Lin, Z.; Hu, S.; Zhou, T.; Zhong, Y.; Zhu, Y.; Shi, L.; Lin, H. Numerical Simulation of Flood Intrusion Process under Malfunction of Flood Retaining Facilities in Complex Subway Stations. *Buildings* **2022**, *12*, 853. [CrossRef]

30. Qin, J.-W.; Liu, C.-C.; Huang, Q. Simulation on fire emergency evacuation in special subway station based on Pathfinder. *Case Stud. Therm. Eng.* **2020**, *21*, 100677. [CrossRef]

31. Shao, Z.-G.; Wang, X.-H.; Yu, D.-H. Study on the simulation of subway station safety evacuation based on Revit Pathfinder. *J. Qingdao Univ. Technol.* **2021**, *42*, 143–148.

32. Zhao, J.-P.; Wang, L. Practical Research on College Students' Increasing Load Running Platform. *Contemp. Sport. Sci. Technol.* **2020**, *10*, 242–244.

33. Kikuchi, T.; Abe, S. Comparison between error correcting output codes and fuzzy support vector machines. *Pattern Recognit. Lett.* **2005**, *26*, 1937–1945. [CrossRef]

34. He, Y.-J.; Tao, Q.-S.; Li, X.-T.; Sun, F.; Zhan, S.-Y. Influence of sex and age on the diagnostic criteria of overweight and obesity in adults. *China Public Health* **2009**, *25*, 441–443.

35. Yang, Y.-Q.; Sun, J.-L.; Jia, L.-Q. Preparation of national Engineering industry standard of Technical Specification for Anti-skid of Building Ground. In *Proceedings of China Building Materials Science and Technology Special Issue of 2013 Floor*; Standards Press of China: Beijing, China, 2000; pp. 66–69.